

PAPER

View Article Online
View Journal | View IssueCite this: *J. Mater. Chem. A*, 2014, 2,
15945Systematic evaluation of HOMO energy levels for
efficient dye regeneration in dye-sensitized solar
cells†Takashi Funaki,^{*ab} Hiromi Otsuka,^b Nobuko Onozawa-Komatsuzaki,^{ab}
Kazuyuki Kasuga,^b Kazuhiro Sayama^{ab} and Hideki Sugihara^{*b}

Thirty ruthenium complexes of the types [Ru(tctpy)(C[^]N)NCS] and [Ru(tctpy)(N[^]O)NCS] (C[^]N = cyclometalating ligand and N[^]O = pyridinecarboxylate and its derivatives) were synthesized and evaluated to identify the highest occupied molecular orbital (HOMO) energy level (E_{HOMO}) for efficient dye regeneration in dye-sensitized solar cells. E_{HOMO} of these complexes was systematically tuned by changing the electron-donating ability of the C[^]N and N[^]O ligands. For complexes with an E_{HOMO} in the potential range more negative than 0.5 V vs. a saturated calomel electrode (SCE), the incident photon-to-current conversion efficiency (IPCE) increased with a positive shift in E_{HOMO} but could not exceed 70%, suggesting that rapid dye regeneration is difficult. On the other hand, high IPCEs above 70% were often observed for complexes with an E_{HOMO} more positive than 0.5 V vs. SCE. It is thus concluded that there is a threshold for efficient electron transfer near 0.5 V vs. SCE ($\Delta G_2 \approx 0.3$ eV) for the series of these sensitizers.

Received 5th February 2014

Accepted 22nd July 2014

DOI: 10.1039/c4ta00613e

www.rsc.org/MaterialsA

Introduction

Dye-sensitized solar cells (DSSCs) have been extensively investigated because of their ease of fabrication and low production costs.¹ Extensive effort has been devoted to the development of new, highly efficient sensitizers, as they play a critical role in cell performance. Of these various sensitizers, [Ru(Hdcbpy)₂-(NCS)₂](TBA)₂ (dcbpy = 4,4'-dicarboxy-2,2'-bipyridine and TBA = tetrabutylammonium) (N719)² and [Ru(Htctpy)(NCS)₃](TBA)₃ (tctpy = 4,4',4''-tricarboxy-2,2':6',2''-terpyridine) (N749)³ are two of the most effective complexes, and DSSCs based on these dyes have achieved a solar-to-electricity conversion efficiency of 11%.^{2,4}

To improve the conversion efficiency of DSSCs, sensitizers exhibiting absorption over a wide range of the solar spectrum and a high molecular extinction coefficient have been investigated. The absorption properties of ruthenium(II) complexes, for example, can be tuned by careful consideration of the highest occupied molecular orbital (HOMO) and lowest unoccupied molecular orbital (LUMO) energy levels.⁵ The absorption

band can be extended to longer wavelengths by destabilizing the metal t_{2g} orbital using a strong donor ligand and/or introducing a ligand with a low-lying π^* -level molecular orbital. To realize high performance solar cells, an enhanced spectral response of the sensitizer in the lower energies is required while maintaining sufficient thermodynamic driving forces for both electron injection and dye regeneration. Systematic tuning of the HOMO and LUMO energy levels (E_{HOMO} and E_{LUMO}) of sensitizers is necessary to estimate the energy difference (ΔG) for sufficient thermodynamic driving forces.

Kato and co-workers reported that a sufficiently high energy difference ($\Delta G_1 > 0.2$ eV) is required to attain efficient electron injection for dye-sensitized ZnO films.⁶ They further quantitatively evaluated ruthenium complexes and organic dyes in dye-sensitized TiO₂ films.⁷ On the other hand, there are several reports on the sufficient energy difference for efficient dye regeneration (ΔG_2). For the case of cobalt and ferrocene redox couples, the dye regeneration kinetics for combination of organic dyes and different redox couples were examined. By varying the redox potential of cobalt complexes, Feldt *et al.* showed that efficient dye regeneration can be achieved with a ΔG_2 of 0.25 eV when a highly concentrated electrolyte is used.⁸ Daenke *et al.* reported that a ΔG_2 of 0.20–0.25 eV for ferrocene redox couples is sufficient to regenerate the dye quantitatively.⁹

For the case of the I_3^-/I^- redox couple with ruthenium complexes, a minimum value of ΔG_2 was reported to be about 0.75 eV.¹⁰ The redox potentials of I_3^-/I^- and I_2^-/I^- in acetonitrile are reported to be 0.11 and 0.55 ± 0.10 V vs. a saturated calomel electrode (SCE), respectively.¹¹ However, Schulze *et al.*

^aResearch Center for Photovoltaic Technologies, National Institute of Advanced Industrial Science and Technology (AIST), AIST Tsukuba Central 5, 1-1-1 Higashi, Tsukuba, Ibaraki 305-8565, Japan. E-mail: takashi-funaki@aist.go.jp; Fax: +81-29-861-4641; Tel: +81-29-861-4892

^bEnergy Technology Research Institute, National Institute of Advanced Industrial Science and Technology (AIST), AIST Tsukuba Central 5, 1-1-1 Higashi, Tsukuba, Ibaraki 305-8565, Japan. E-mail: sugihara-hideki@aist.go.jp; Tel: +81-29-861-6273

† Electronic supplementary information (ESI) available. See DOI: 10.1039/c4ta00613e

suggested that approximately 0.66 V *vs.* SCE is required for efficient dye regeneration,¹² and Islam *et al.* suggested that sensitizers should possess an E_{HOMO} greater than 0.53 V *vs.* SCE.¹³ We reported that there seems to be a threshold for rapid dye regeneration near 0.5 V *vs.* SCE.¹⁴ It is essential to know the required difference between the E_{HOMO} of a sensitizer and the iodine redox potential to design highly efficient sensitizers.

Herein we investigate the influence of E_{HOMO} on the dye regeneration process in detail. Thirty ruthenium complexes of the types [Ru(tctpy)(C[^]N)NCS] and [Ru(tctpy)(N[^]O)NCS] (C[^]N = cyclometalating ligand and N[^]O = pyridinecarboxylate and its derivatives) were synthesized. The introduction of C[^]N and N[^]O ligands made it possible to tune the E_{HOMO} of the resulting complexes while maintaining an E_{LUMO} for efficient electron injection into the conduction band of a TiO₂ electrode. By changing the electron-donating ability of the C[^]N and N[^]O ligands, the E_{HOMO} of each of the resulting complexes was systematically tuned. The molecular structures of the prepared ruthenium complexes with E_{HOMO} values ranging from 0.33 to 0.77 V *vs.* SCE are shown in Fig. 1.

Experimental

General

Commercially available chemicals and solvents were used as received. Microwave irradiation reactions were carried out using a CEM Discover microwave synthesizer and reaction temperatures were monitored using an equipped IR sensor. Nuclear magnetic resonance (NMR) spectra were obtained on a Varian INOVA 400 spectrometer, a Bruker Avance 400 spectrometer, a Bruker Avance 500 spectrometer, and a JEOL JNM-LA 600 spectrometer. Chemical shifts are given in ppm relative to standard. Electrospray ionization mass spectra (ESI-MS) were recorded on a Waters ZQ mass spectrometer. Cyclic voltammograms and differential pulse voltammograms were collected using a BAS-100 electrochemical analyzer (Bioanalytical System). The photovoltaic measurements were performed using a Xe lamp light source simulating the AM 1.5 spectrum (Wacom, WXS-80C-2, 100 mW cm⁻²). The incident photon-to-current conversion efficiency (IPCE) was measured using an Eko Seiki SPM-005B equipped with a Xe lamp and a halogen lamp.

Synthesis

Details on the synthesis of C[^]N ligands and ruthenium complexes are provided in the ESI.†

Electrochemical studies

Cyclic voltammograms and differential pulse voltammograms of the ruthenium complexes were measured in a solution containing 0.1 M lithium perchlorate using a three-electrode apparatus comprising a platinum wire counter electrode, a platinum working electrode, and a Ag/AgCl (saturated aqueous KCl) reference electrode in contact with a NaCl salt bridge. Complexes 1–23, N719, and N749 were dissolved in *N,N*-dimethylformamide at a concentration of 1×10^{-3} M, and complexes 24–30 were dissolved in methanol at a concentration

of 1×10^{-3} M. Ferrocene was added to each sample solution at the end of the experiment, and a ferrocenium/ferrocene redox couple (0.39 V *vs.* SCE) was used as an internal potential reference.

Photovoltaic performance

Nanocrystalline TiO₂ films (area: 0.25 cm²; thickness: 38 μm) were prepared *via* screen printing on conductive glass (Nippon Sheet Glass Co., Japan, F-doped SnO₂ layer) as described previously.¹⁵ The TiO₂ films were heated to 525 °C for 1 h in air and then allowed to cool to 120 °C before being dipped in 0.1 M HCl at 80 °C for 2 h. After rinsing with water and ethanol, the TiO₂ photoelectrodes were immersed in a dye solution for 22 h at 25 °C. We tried to find conditions giving the highest short-circuit current density. Therefore, the concentration was different between 1–23 and 24–30. Complexes 1–23 were dissolved in ethanol (2×10^{-4} M) containing 4×10^{-4} M TBA(OH) and 2×10^{-2} M deoxycholic acid (DCA), whereas complexes 24–30 were dissolved in ethanol (1×10^{-4} M) containing 2×10^{-4} M TBA(OH) and 1×10^{-2} M DCA. Although the concentrations were different, the molar ratio of 1–30 to DCA is 1 : 100. N749 was dissolved only in ethanol (2×10^{-4} M), and N719 was dissolved in a mixed solution of acetonitrile and *tert*-butyl alcohol (1 : 1, v/v; 3×10^{-4} M). Photoelectrochemical measurements were performed using a two-electrode solar cell consisting of the dye-coated TiO₂ electrode, a platinum film counter electrode, a polypropylene film spacer (thickness: 60 μm), and an electrolyte solution consisting of 0.6 M 1,2-dimethyl-3-propylimidazolium iodide, 0.05 M iodine, 0.1 M lithium iodide, and 0 or 0.5 M *tert*-butylpyridine (TBP) in acetonitrile.

Results and discussion

The synthesis of complexes 1–23 of the type [Ru(tctpy)(C[^]N)NCS] is shown in Scheme 1. For complexes 1–18, the cyclometalation step was conducted in EtOH–water (3 : 1, v/v), whereas for complexes 19–23, both the cyclometalation step and the hydrolysis of the ester group occurred in DMF–water (3 : 1, v/v) at an elevated temperature. Complexes 1–23 should exist as mixtures of stereoisomers; however, it was possible to obtain the single isomer depicted in Scheme 1 using a microwave synthetic technique. The structures of the resulting complexes were identified *via* NMR and ESI-MS analysis. The most upfield signal in the aromatic region of the NMR spectra, which is assigned to the proton at the *ortho* position to the organometallic bond, is useful spectroscopic evidence for cyclometalation.¹⁶ The further upfield shift of this proton in the NMR spectra of the obtained single isomers is due to the ring current effect of the 2,2':6',2''-terpyridine ligand.¹⁷

The synthesis of complexes 24–28 of the type [Ru(tctpy)(N[^]O)NCS] is shown in Scheme 2. Complexes 24–28 were prepared as mixtures of stereoisomers, but it was possible to obtain the single isomer depicted in Scheme 2 as a pure compound using column chromatography. Complexes 29 and 30 were also synthesized using the procedure shown in Scheme 2. However, they exist as stereoisomers with the relative disposition of the

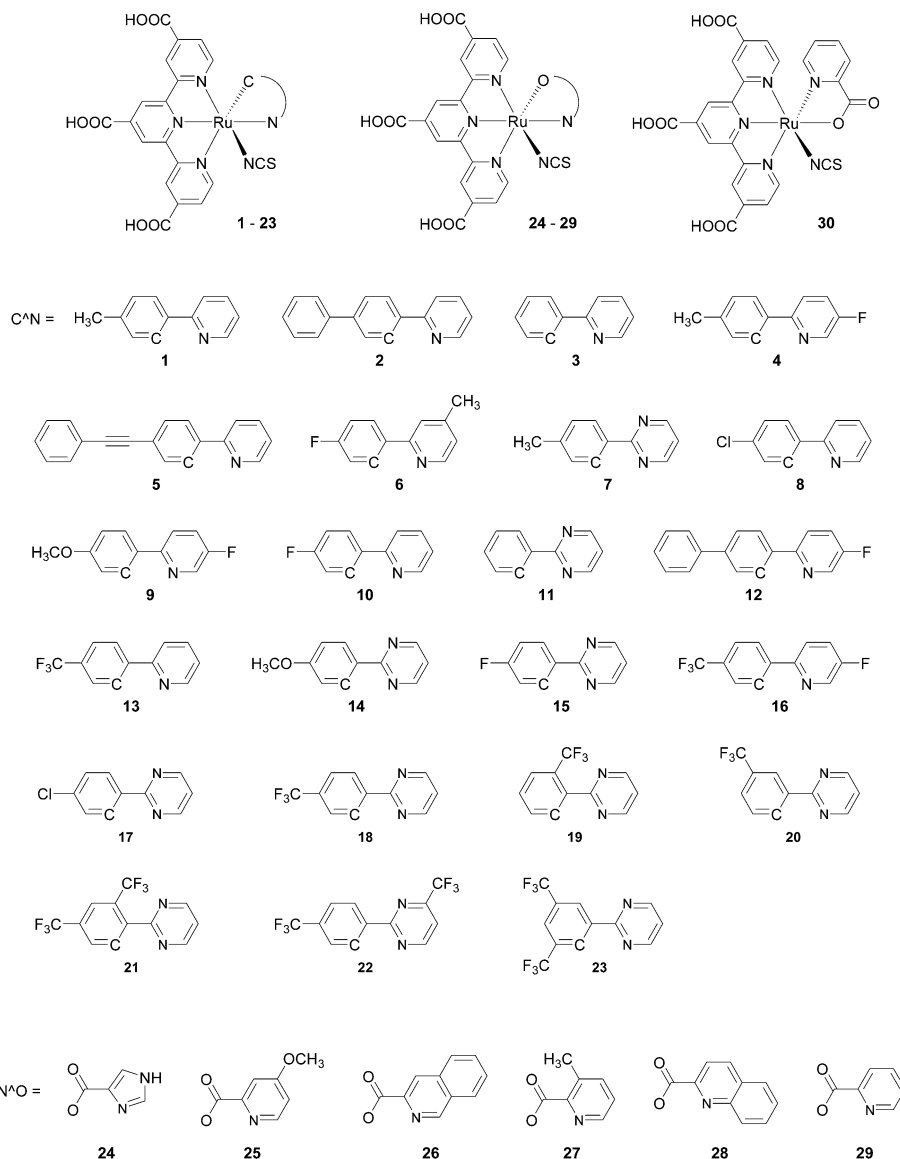
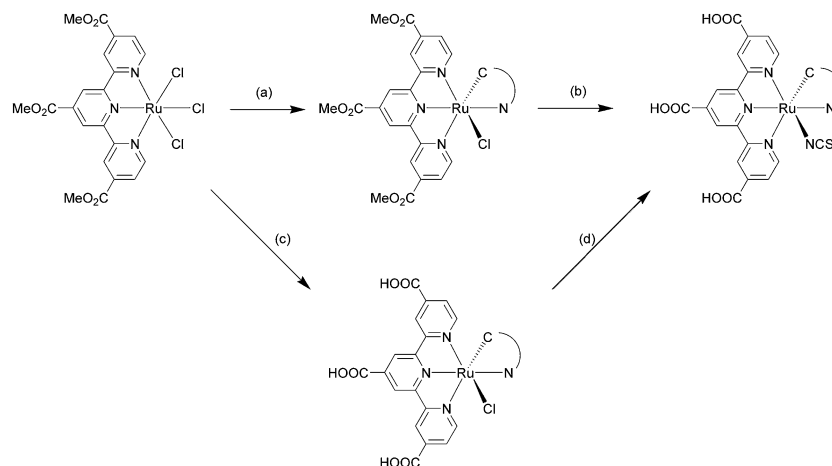


Fig. 1 Molecular structures of ruthenium complexes.

pyridyl group on the N^O ligand and the central pyridyl group on the 2,2':6',2''-terpyridine ligand differing for each isomer. Each isomer was identified *via* ¹H NMR analysis. For complex 29, the most downfield signal (δ 9.37 ppm) is assigned to the proton in the 6-position of the pyridyl group, which is close to the NCS group.¹⁸ On the other hand, the signal of the proton in the 6-position of the pyridyl group of 30 (δ 6.74 ppm) is upfield shifted, probably due to the ring current effect of the 2,2':6',2''-terpyridine ligand.

Cyclic voltammetry and differential pulse voltammetry (DPV) were then performed to determine the E_{HOMO} of the ruthenium complexes. A quasi-reversible wave for the Ru^{3+/2+} couple was obtained, and the peak potentials of the differential pulse voltammograms for 1–30, N719, and N749 are listed in Table 1. Typical DPV spectra of ruthenium complexes and the electrolyte (I₃[−]/I[−]) are shown in Fig. S1.† Under the experimental conditions employed, the peak potential for DPV of I₃[−]/I[−] was 0.23 V

vs. SCE (Fig. S1†). Therefore, the ΔG_2 values of 1–30, N719, and N749 are also listed in Table 1. The redox potentials for complexes 1–30 were strongly affected by the introduction of the C^N and N^O ligands. The negative shift in the E_{HOMO} of complexes 1–23 relative to that of N749 (0.66 V *vs.* SCE) was attributed to the introduction of the C^N ligand, because cyclometalating ligands have a strong electron-donating ability. On the other hand, because the electron-donating ability of the single 2-pyridinecarboxylate ligand is inferior to that of two isothiocyanate ligands,^{5a} the E_{HOMO} of complexes 24–30 was positively shifted. Moreover, structural modification of the C^N and N^O ligands had an effect on the electrochemical properties of the resulting complexes. For example, a positive shift in the E_{HOMO} of 8 relative to that of 3 was attributed to the introduction of the electron-withdrawing substituent on the C^N ligand, which decreased its electron-donating ability. In contrast, a negative shift in the E_{HOMO} was observed when



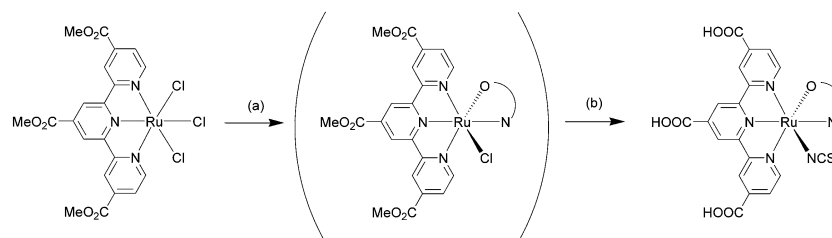
Scheme 1 Synthesis of **1–23**: (a) 2-phenylpyridine or a derivative, Et₃N, EtOH, H₂O. (b) 1. NH₄SCN, DMF, H₂O, microwave. 2. Et₃N. (c) Derivative of 2-phenylpyrimidine, Et₃N, DMF, H₂O, microwave. (d) NH₄SCN, DMF, H₂O, microwave.

electron-donating substituents were introduced. Thus, the E_{HOMO} was systematically tuned by changing the substituents of the ligands.

The photovoltaic performance of the DSSCs under standard air mass 1.5 irradiation (100 mW cm⁻²) conditions is shown in Table 1. We tried to find conditions giving the highest short-circuit current density (J_{sc}). Therefore, an electrolyte without TBP was used for the cells based on complexes **24–30** because the E_{LUMO} of each of these complexes was relatively close to the TiO₂ conduction band edge.¹⁹ The open-circuit voltage (V_{oc}) values for the DSSCs based on complexes **24–30** were lower than those for **N719** and **N749** due to a shift of the TiO₂ conduction band edge (Fig. 2(b)). It has been reported that the addition of TBP or a similar compound to the electrolyte increases the V_{oc} of DSSCs by shifting the conduction band of TiO₂ to more negative potentials.²⁰ Furthermore, it should be noted that the efficiency of complexes **28–30** was slightly lower than that reported previously,¹⁹ for which the photovoltaic performance data were obtained for cells using an electrolyte solution with TBP (0.2 or 0.1 M). The efficiency of **11**, **18**, and **21** was also lower than that reported previously because these data were obtained using sealed cells with an antireflection film and a black metal mask.¹⁴ The efficiency of **11**, **15**, and **18–23** was similar to that reported previously,²¹ for which the data were obtained using cells with different TiO₂ films (thickness: 31 μm).

As shown in Fig. 2, J_{sc} , open-circuit voltage (V_{oc}), and overall conversion efficiency (η) of the cells based on complexes **1–23** increased as the ΔG_2 increased. These findings suggest that the E_{HOMO} of ruthenium complexes strongly affects the photovoltaic performance of DSSCs when the E_{HOMO} is less than 0.5 V vs. SCE. When the ΔG_2 is small, rapid dye regeneration is difficult because of an insufficient driving force. The J_{sc} , V_{oc} , and η values decreased as the energy difference decreased, most likely because the ratio of charge recombination increased. The energy matching between the HOMO and the iodine redox mediator is crucial for attaining high-performance DSSCs. At this point, it remains unclear whether other parameters, such as the molecular structure and interactions of the dye with the electrolyte solution components, affect the efficiency of dye regeneration. However, given the similar structures of complexes **1–23**, the low J_{sc} , V_{oc} , and η values for the DSSCs based on **1–12** (0.33–0.42 V vs. SCE) were mainly attributed to an insufficient driving force for rapid dye regeneration.

Fig. 3 shows the relationship between the maximum IPCE values (IPCE_{max}) of the DSSCs and the E_{HOMO} and ΔG_2 values of the ruthenium complexes for estimation of the appropriate E_{HOMO} for rapid dye regeneration. The IPCE spectra of the DSSCs based on the ruthenium complexes are shown in Fig. S3.† As depicted in Fig. S2,† molecular extinction coefficients (ϵ) of ruthenium complexes are slightly different. To compensate for the low ϵ of the ruthenium complexes, very



Scheme 2 Synthesis of **24–28**: (a) derivative of 2-pyridinecarboxylic acid, LiCl, Et₃N, EtOH. (b) 1. NH₄SCN, DMF, H₂O. 2. Et₃N.

Table 1 Electrochemical data and photovoltaic performance of DSSCs

Complexes	E_{HOMO} /V vs. SCE	ΔG_2 /eV	IPCE _{max} /%	TBP/M	J_{sc}^a /mA cm ⁻²	V_{oc}^b /mV	ff ^c	η^d /%
1	0.33	0.10	28	0.5	4.4	0.51	0.69	1.5
2	0.33	0.10	43	0.5	9.1	0.57	0.70	3.6
3	0.37	0.14	32	0.5	6.1	0.53	0.69	2.2
4	0.37	0.14	29	0.5	4.6	0.52	0.71	1.7
5	0.38	0.15	41	0.5	9.1	0.58	0.70	3.7
6	0.39	0.16	45	0.5	9.6	0.56	0.70	3.8
7	0.39	0.16	32	0.5	6.3	0.54	0.73	2.5
8	0.40	0.17	45	0.5	10.8	0.57	0.70	4.3
9	0.40	0.17	32	0.5	5.6	0.53	0.72	2.1
10	0.42	0.19	45	0.5	11.0	0.56	0.69	4.3
11	0.42	0.19	40	0.5	7.7	0.54	0.72	3.0
12	0.42	0.19	40	0.5	8.3	0.55	0.70	3.2
13	0.43	0.20	59	0.5	16.0	0.62	0.68	6.9
14	0.43	0.20	32	0.5	6.7	0.55	0.72	2.7
15	0.48	0.25	61	0.5	15.4	0.61	0.68	6.4
16	0.48	0.25	57	0.5	15.8	0.63	0.69	6.8
17	0.48	0.25	49	0.5	12.4	0.59	0.70	5.2
18	0.49	0.26	65	0.5	18.3	0.62	0.68	7.7
19	0.49	0.26	69	0.5	20.2	0.65	0.66	8.6
20	0.51	0.28	71	0.5	21.5	0.64	0.65	8.9
21	0.52	0.29	74	0.5	21.3	0.69	0.68	9.9
22	0.55	0.32	73	0.5	20.3	0.68	0.68	9.4
23	0.56	0.33	75	0.5	20.0	0.70	0.67	9.3
24	0.61	0.38	62	0	15.7	0.53	0.71	5.9
25	0.65	0.42	76	0	20.3	0.53	0.68	7.3
26	0.68	0.45	65	0	19.0	0.55	0.66	6.9
27	0.69	0.46	80	0	21.5	0.55	0.67	8.0
28	0.71	0.48	73	0	19.9	0.52	0.66	6.8
29	0.73	0.50	73	0	18.8	0.55	0.69	7.1
30	0.77	0.54	62	0	13.8	0.54	0.71	5.3
N719	0.85	0.62	77	0.5	16.6	0.73	0.74	8.9
N749	0.66	0.43	71	0.5	19.6	0.71	0.69	9.6

^a Short-circuit current density. ^b Open-circuit voltage. ^c Fill factor. ^d Overall solar light-to-electrical conversion efficiency.

thick TiO₂ films (38 μm) were used in this study. Furthermore, to obtain a sufficient thermodynamic driving force for electron injection, an electrolyte without TBP was used for the cells based on complexes **24**–**30**. The efficiency of dye regeneration is an important factor determining the electron collection efficiency. After electron injection, a competition is established between dye regeneration and charge recombination. If the thermodynamic driving force for dye regeneration is insufficient, charge recombination dominates, resulting in a low IPCE_{max} for the DSSC. The ratio of charge recombination increases when the E_{HOMO} shifts toward more negative potentials.

As can be seen in Fig. 3, the IPCE_{max} increased with a positive shift in the E_{HOMO} for the complexes with an E_{HOMO} in the potential range more negative than 0.5 V vs. SCE, but did not exceed 70%, suggesting that rapid dye regeneration is difficult. The reduced IPCE_{max} is probably due to a decrease in the driving force for dye regeneration. On the other hand, a high IPCE_{max} above 70% was often observed for the complexes with an E_{HOMO} more positive than 0.5 V vs. SCE. It can thus be concluded that there is a threshold for efficient electron transfer near 0.5 V vs. SCE ($\Delta G_2 \approx 0.3$ eV) in the series of these sensitizers. Notably, the cell based on complex **20** exhibited an

IPCE_{max} of 71%, although the E_{HOMO} of **20** was 0.34 and 0.15 eV more negative than that of **N719** and **N749**, respectively.

At present, the reason for the relatively small IPCE_{max} values of complexes **24**, **26**, and **30** is not clear. It is possible that the molecular structures and interactions of the dyes with the electrolyte solution affect the efficiency of dye regeneration. Indeed, there are several sensitizers with similar E_{HOMO} values but different IPCE_{max} in complexes **1**–**23**. Thus, deviation seems to be similar for whole complexes. The origin of the deviation is not clear, but it could be related to the different substituent groups on the C[^]N and N[^]O ligands. Complexes **1**–**23** have several types of electron-donating and electron-withdrawing groups on the C[^]N ligands, and the influence of these groups is shown in Fig. S4.† These results suggest that higher IPCE_{max} values were obtained for complexes with ligands bearing an electron-withdrawing substituent. In addition, the tri-fluoromethyl group seems to be a particularly effective electron-withdrawing group.

Although several factors may affect dye regeneration, the energy difference between the HOMO and the iodine redox mediator is one of the most important factors. To realize high performance solar cells, an enhanced spectral response of the sensitizer at lower energies is required while maintaining a

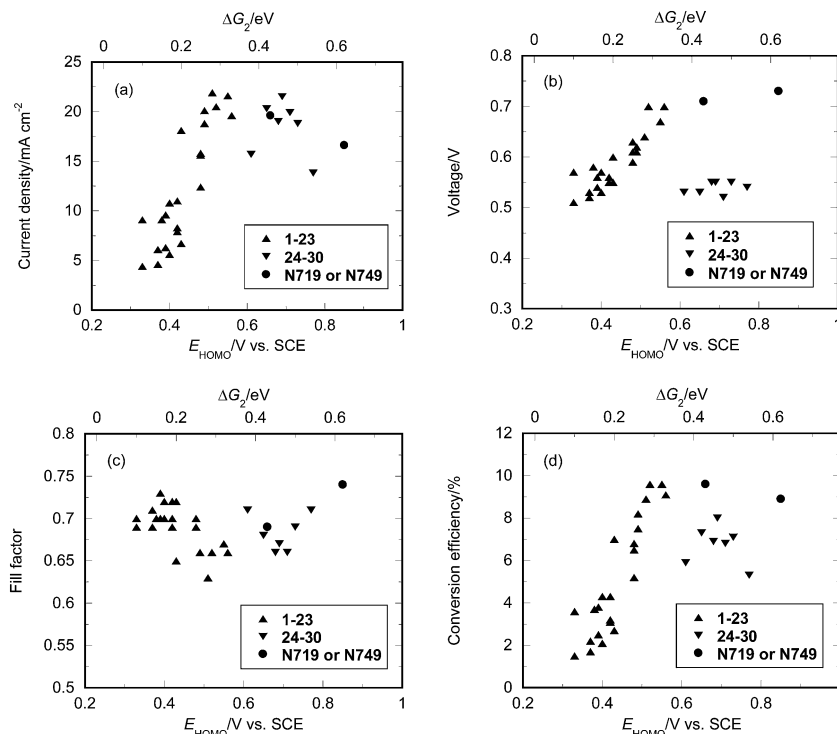


Fig. 2 (a) Short-circuit current density, (b) open-circuit voltage, (c) fill factor, and (d) overall conversion efficiency of DSSCs as a function of the E_{HOMO} and ΔG_2 of ruthenium complexes.

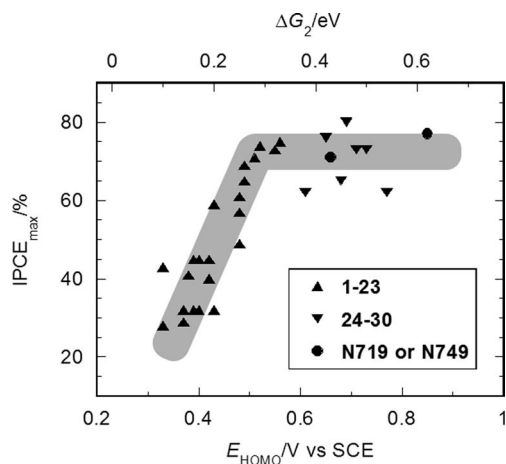


Fig. 3 Maximum IPCE values for DSSCs as a function of the E_{HOMO} and ΔG_2 of ruthenium complexes.

sufficient thermodynamic driving force for dye regeneration. Because DPV is a general analytical method, it can be a useful tool for the optimization of the E_{HOMO} of newly synthesized sensitizers under the same conditions.

Conclusion

We have synthesized thirty ruthenium complexes to elucidate the E_{HOMO} required for efficient dye regeneration in DSSCs. The introduction of C[^]N and N[^]O ligands made it possible to tune the E_{HOMO} of the resulting complexes while maintaining an

E_{LUMO} for efficient electron injection into the conduction band of a TiO_2 electrode. Structural modification of the ligands greatly influenced the E_{HOMO} and enabled systematic tuning. For complexes with an E_{HOMO} in the potential range more negative than 0.5 V vs. SCE, the IPCE increased with a positive shift in E_{HOMO} , but did not exceed 70%, suggesting that rapid dye regeneration is difficult. On the other hand, high IPCEs above 70% were often observed for complexes with an E_{HOMO} more positive than 0.5 V vs. SCE. It is thus concluded that there is a threshold for efficient electron transfer near 0.5 V vs. SCE ($\Delta G_2 \approx 0.3$ eV) in the series of these sensitizers. The present study provides a new criterion for sensitizer designs, because it is important to minimize the energy difference between the HOMO and the iodine redox mediator. We believe that these findings will thus enable the design of highly efficient sensitizers.

Acknowledgements

This research was partly supported by the Japan Society for the Promotion of Science (JSPS) through its "Funding Program for World-Leading Innovative R&D on Science and Technology" (FIRST Program). We are grateful to Prof. Dr S. Mori from Shinshu University for valuable discussion.

References

- (a) B. O'Regan and M. Grätzel, *Nature*, 1991, **353**, 737; (b) M. Grätzel, *Acc. Chem. Res.*, 2009, **42**, 1788; (c) A. Hagfeldt,

- G. Boschloo, L. Sun, L. Kloo and H. Pettersson, *Chem. Rev.*, 2010, **110**, 6595.
- 2 (a) M. K. Nazeeruddin, A. Key, I. Rodicio, R. Humphry-Baker, E. Müller, P. Liska, N. Vlachopoulos and M. Grätzel, *J. Am. Chem. Soc.*, 1993, **115**, 6382; (b) M. K. Nazeeruddin, F. De Angelis, S. Fantacci, A. Selloni, G. Viscardi, P. Liska, S. Ito, B. Takeru and M. Grätzel, *J. Am. Chem. Soc.*, 2005, **127**, 16835.
- 3 M. K. Nazeeruddin, P. Péchy, T. Renouard, S. M. Zakeeruddin, R. Humphry-Baker, P. Comte, P. Liska, L. Cevey, E. Costa, V. Shklover, L. Spiccia, G. B. Deacon, C. A. Bignozzi and M. Grätzel, *J. Am. Chem. Soc.*, 2001, **123**, 1613.
- 4 Y. Chiba, A. Islam, Y. Watanabe, R. Komiya, N. Koide and L. Han, *Jpn. J. Appl. Phys.*, 2006, **45**, L638.
- 5 (a) K. Kalyanasundaram and M. K. Nazeeruddin, *Chem. Phys. Lett.*, 1992, **193**, 292; (b) P. A. Anderson, G. F. Strouse, J. A. Treadway, F. R. Keene and T. J. Meyer, *Inorg. Chem.*, 1994, **33**, 3863; (c) M. K. Nazeeruddin and M. Grätzel, *Compr. Coord. Chem. II*, 2003, **9**(Chap. 16), 719.
- 6 R. Katoh, A. Furube, K. Hara, S. Murata, H. Sugihara, H. Arakawa and M. Tachiya, *J. Phys. Chem. B*, 2002, **106**, 12957.
- 7 R. Katoh, *Ambio*, 2012, **41**, 143.
- 8 S. M. Feldt, P. W. Lohse, F. Kessler, M. K. Nazeeruddin, M. Grätzel, G. Boschloo and A. Hagfeldt, *Phys. Chem. Chem. Phys.*, 2013, **15**, 7087.
- 9 T. Daeneke, A. J. Mozer, Y. Uemura, S. Makuta, M. Fekete, Y. Tachibana, N. Koumura, U. Bach and L. Spiccia, *J. Am. Chem. Soc.*, 2012, **134**, 16925.
- 10 G. Boschloo and A. Hagfeldt, *Acc. Chem. Res.*, 2009, **42**, 1819.
- 11 G. Boschloo, E. A. Gibson and A. Hagfeldt, *J. Phys. Chem. Lett.*, 2011, **2**, 3016.
- 12 B. Schulze, D. G. Brown, K. C. D. Robson, C. Friebe, M. Jäger, E. Birkner, C. P. Berlinguette and U. S. Schubert, *Chem.-Eur. J.*, 2013, **19**, 14171.
- 13 A. Islam, S. P. Singh and L. Han, *Int. J. Photoenergy*, 2011, 204639.
- 14 T. Funaki, H. Funakoshi, N. Onozawa-Komatsuzaki, K. Kasuga, K. Sayama and H. Sugihara, *Angew. Chem., Int. Ed.*, 2012, **51**, 7528.
- 15 Z.-S. Wang, H. Kawauchi, T. Kashima and H. Arakawa, *Coord. Chem. Rev.*, 2004, **248**, 1381.
- 16 (a) E. C. Constable and J. M. Holmes, *J. Organomet. Chem.*, 1986, **301**, 203; (b) E. C. Constable and T. A. Leese, *J. Organomet. Chem.*, 1987, **335**, 293; (c) P. G. Bomben, K. D. Thériault and C. P. Berlinguette, *Eur. J. Inorg. Chem.*, 2011, 1806; (d) K. C. D. Robson, B. D. Koivisto, A. Yella, B. Sporinova, M. K. Nazeeruddin, T. Baumgartner, M. Grätzel and C. P. Berlinguette, *Inorg. Chem.*, 2011, **50**, 5494; (e) K. C. D. Robson, B. Sporinova, B. D. Koivisto, E. Schott, D. G. Brown and C. P. Berlinguette, *Inorg. Chem.*, 2011, **50**, 6019.
- 17 T. Funaki, M. Yanagida, N. Onozawa-Komatsuzaki, K. Kasuga, Y. Kawanishi, K. Sayama and H. Sugihara, *Inorg. Chem. Commun.*, 2009, **12**, 842.
- 18 S. M. Zakeeruddin, M. K. Nazeeruddin, P. Pechy, F. P. Rotzinger, R. Humphry-Baker, K. Kalyanasundaram, M. Grätzel, V. Shklover and T. Haibach, *Inorg. Chem.*, 1997, **36**, 5937.
- 19 (a) T. Funaki, M. Yanagida, N. Onozawa-Komatsuzaki, K. Kasuga, Y. Kawanishi and H. Sugihara, *Inorg. Chim. Acta*, 2009, **362**, 2519; (b) T. Funaki, M. Yanagida, N. Onozawa-Komatsuzaki, K. Kasuga, Y. Kawanishi and H. Sugihara, *Chem. Lett.*, 2009, **38**, 62.
- 20 (a) H. Kusama and H. Arakawa, *J. Photochem. Photobiol., A*, 2003, **160**, 171; (b) G. Boschloo, L. Hagman and A. Hagfeldt, *J. Phys. Chem. B*, 2006, **110**, 13144; (c) H. Kusama, H. Orita and H. Sugihara, *Sol. Energy Mater. Sol. Cells*, 2008, **92**, 84.
- 21 H. Kusama, T. Funaki and K. Sayama, *J. Photochem. Photobiol., A*, 2013, **272**, 80.